Environmental Technology & Innovation 35 (2024) 103676

Contents lists available at ScienceDirect

Environmental Technology & Innovation

journal homepage: www.elsevier.com/locate/eti

Operation and integration of a commercially available nitrate sensor in Gulf of Mexico estuarine monitoring programs

Jennifer M. Raabe [a], Gulce Kurtay [a,d], Amanda Fontenot [b], Sierra Greene [c], A.J. Martignette [c], Eric C. Milbrandt [c], Brian J. Roberts [b], Beth A. Stauffer [a,*]

[a] Department of Biology, University of Louisiana at Lafayette, Lafayette, LA, United States
[b] Louisiana Universities Marine Consortium, Chauvin, LA, United States
[c] Marine Laboratory, Sanibel-Captiva Conservation Foundation, Sanibel, FL, United States
[d] The Cooperative Institute for Climate, Ocean, and Ecosystem Studies, University of Washington, Seattle, WA, United States

ARTICLE INFO

Keywords:
Observing systems
Water quality
High frequency
Runoff
Pollution

ABSTRACT

Many coastal and estuarine environments suffering from eutrophication, hypoxia, and harmful algal blooms need continuous nutrient monitoring to better understand the drivers of these events and evaluate progress towards water quality improvement targets. Many dissolved-nutrient sensors are now commercially available with several being evaluated in terms of relative accuracy, precision, limits of detection, and measurement range. There remains a need to test integration of these sensors into existing water quality monitoring programs. This study tested the operational status and integration of a commercial, in situ chemical analyzer for nitrate in two existing monitoring programs in Louisiana and Florida as a pilot study for the development of a nutrient monitoring program across Gulf of Mexico estuaries. Both sites deployed the same sensor, but with slightly altered equipment configurations which resulted in large differences in the duration of data, with 161 (out of 353) days of data collected in Florida compared to 26 (out of 228) days of data in Louisiana. Sensors were also exposed to different nitrate regimes in Florida (mean = 8.94 μM; max = 23.9 μM) versus Louisiana (mean = 2.66 μM; max = 12.9 μM), and site-specific relationships between sensor and reference data were apparent. Also highlighted are the needs to address integrating new sensors into existing monitoring infrastructure including full interoperability with non-proprietary datalogger systems and ongoing needs for more site-specific calibrations and post-hoc corrections. Addressing these needs will help ensure successful integration into existing monitoring infrastructure and availability of continuous nutrient data.

1. Introduction

Nutrient pollution is an ongoing challenge for water quality worldwide. While much of the problem originates in inland watersheds, many of the effects are seen in coastal and estuarine waters that experience eutrophication (Maure et al., 2021), harmful algal blooms (HABs; Glibert et al., 2018; Medina et al., 2022), and hypoxia (Breitburg et al., 2018; Howarth et al., 2011). High-nutrient runoff from agricultural lands (Withers et al., 2014) and urban areas (Tromboni and Dodds, 2017; Wurtsbaugh et al., 2019) are the main causes of coastal eutrophication (Paerl et al., 1998) which can stimulate harmful algal blooms (HABs) that cause millions of

* Corresponding author.
E-mail address: beth.stauffer@louisiana.edu (B.A. Stauffer).

https://doi.org/10.1016/j.eti.2024.103676
Received 28 December 2023; Received in revised form 29 April 2024; Accepted 13 May 2024
Available online 14 May 2024

dollars in damages annually (Hamilton et al., 2009; Heil and Muni-Morgan, 2021; Kouakou and Poder, 2019; Smith et al., 2019), and accelerated deoxygenation of the coastal ocean (Harrison et al., 2017; Young et al., 2020). In the northern Gulf of Mexico (GoM), an annually recurring 'dead zone', a direct result of nitrogen pollution from the Mississippi Atchafalaya River Basin (Rabalais and Turner, 2001; Rabalais et al., 1999, 2002; Robertson and Saad, 2013), negatively impacts the economics of fisheries (Craig, 2012; Craig et al., 2005; Purcell et al., 2017).

Enhanced nutrient monitoring is required to support research and management to assess the effectiveness of upstream nutrient reduction efforts on coastal water quality. For example, the predictive models used to estimate the areal extent of GoM hypoxia each year depend on spring nitrate loads (Scavia et al., 2003; Turner et al., 2006, 2012) which have historically been based on discrete water sample collection and estimation techniques (Pellerin et al., 2014). However, sensor-based, continuous measurements of nutrient concentrations improve the accuracy of monthly NO_3^- loads and can therefore produce improved predictions of the size of the hypoxia zone (Pellerin et al., 2014; Scavia et al., 2003; Turner et al., 2006). A nutrient sensor network within the northern GoM can also help guide the US EPA Mississippi River/Gulf of Mexico Hypoxia Task Force on their goal to reduce the five-year average area of the Gulf of Mexico hypoxic zone to $< 5000\ km^2$ (USEPA, 2013)

Long-term continuous monitoring can be achieved by using high frequency, in situ nutrient sensors. Commercially available nutrient sensors take two main forms at present: optical sensors that measure nutrients based on absorbance in the environment and wet chemistry analyzers (Daniel et al., 2020). However, it should be noted that wet chemistry analyzers also use internal optical sensors (i.e., spectrometers) to measure endpoints of the colorimetric reactions that are converted to measured concentrations (Daniel et al., 2020).

Optical sensors use ultraviolet (UV) spectrophotometry to measure nitrate concentrations and typically have short response times (Daniel et al., 2020; Meyer et al., 2018; Pellerin et al., 2016). Additionally, the UV sensor, SUNA (Sea-Bird Scientific, Bellevue, Washington, United States), is capable of long-term, unattended deployment for over a year at a measurement frequency of five samples per day (Johnson and Coletti, 2002). They also have a large nitrate measurement range of 0.5–3200 μM but are susceptible to optical interferences (Daniel et al., 2020; Meyer et al., 2018; Pellerin et al., 2013). Optical sensors remain more expensive to purchase than wet chemical sensors and often require sophisticated data processing to yield nutrient concentrations, although savings in

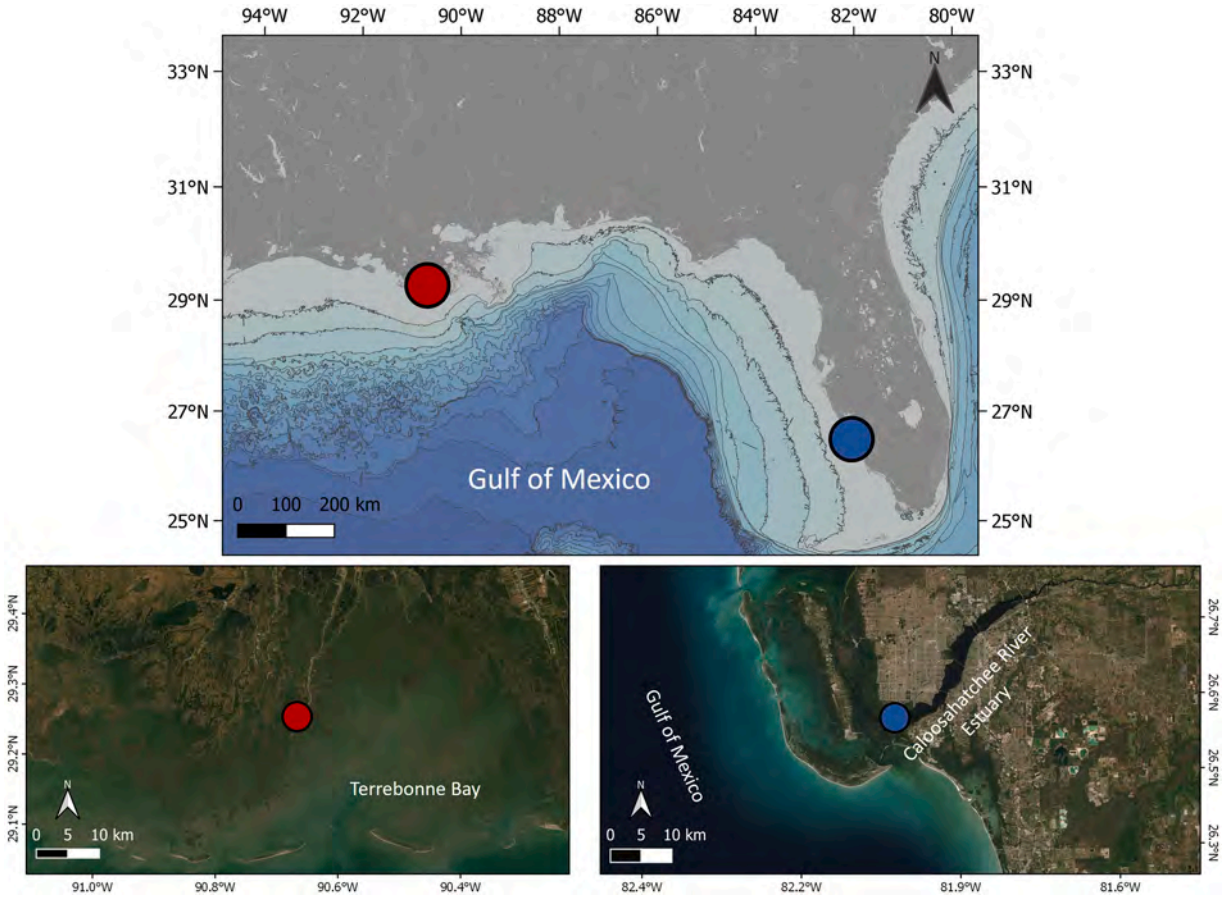

Fig. 1. Map of the study locations. Top map includes the entirety of the study area with LUMCON (red circle) and SCCF (blue circle). Bottom left map is satellite imagery of the LUMCON deployment site (red circle) in northern Terrebonne Bay, Louisiana. Bottom right map is satellite imagery of the SCCF deployment site (blue circle) just at the mouth of the Caloosahatchee River within the Caloosahatchee River Estuary.

reagents and other operational needs may offset initial costs.

Wet chemistry sensors typically require more power, involve the consumption of reagents for analyses, and are often larger and heavier given the need to carry reagents onboard (Daniel et al., 2020; Grand et al., 2017; Pellerin et al., 2016). However, they typically have high accuracy and precision, and are able to detect trace levels of nitrate (0.02 μM; see Daniel et al., 2020) and other nutrient targets (i.e., phosphate, ammonium, silica) either alone or in combination (e.g., Copetti et al., 2014; Moscetta et al., 2009). Recent improvements in wet chemical analyzers for nitrate use the VCl_3 reduction method which minimizes sample volume and use of toxic chemicals and results in fewer interferences (Schnetger and Lehners, 2014; Wang et al., 2016).

Nutrient sensor technologies are powerful tools for addressing national and global needs for monitoring and improvement of water quality. In 2015–2016, six models of commercially-available sensors were tested for performance in measuring nitrate and phosphate by the Alliance for Coastal Technologies (ACT) as part of the U.S. interagency Nutrient Sensor Challenge (https://www.act-us.info/nutrients-challenge/). Sensors were evaluated for accuracy and precision, limits of detection (LOD), ease of use, and costs to operate and maintain (https://www.act-us.info/evaluations.php#Nut2). The winner of the Nutrient Sensor Challenge Nitrate category was Systea s.P.A. (Anagni, Italy) with the wet chemical Water In-Situ Analyzer, or WIZ probe. The current study builds upon the verification testing of these sensors, which was carried out in controlled lab conditions, facilitated by manufacturer technicians in the field, and with stand-alone systems not tasked with providing real-time data. The current study explicitly tests the operational status and integration of the WIZ in two existing estuarine monitoring programs in the GoM.

Operational status of a sensor can be coarsely defined by the technology readiness level (TRL), a scale that describes different phases (1–9) of technology development (Mankins, 1995). Commercialization of technologies is expected at TRL 8 after the technology has been qualified through testing and demonstrations (Schierenbeck and Smith, 2017). However, integration of this new generation of wet chemistry analyzer sensors into existing monitoring programs has not been systematically documented. The results of this study provide important data on sensor operation, recommend best practices, and provide guidance for users in selecting and deploying instrumentation. This study also informs developers on how to improve upon existing sensor technology towards better integration. Using lessons learned from this study, and others, a community of practice can build a network of continuous nutrient sensors that capture temporal dynamics, assess nutrient reduction strategies, and ultimately manage coastal natural resources affected by nutrient pollution.

2. Materials and methods

2.1. Study region and site descriptions

Commercially available, high frequency in situ wet chemical sensors for nitrate inclusive of nitrite ($NO_3^- + NO_2^-$, hereafter referred to as "nitrate") were deployed at two estuarine sites in the GoM (Fig. 1). The GoM is also home to a number of ongoing coastal and estuarine programs monitoring the dynamics of these downstream effects of nutrient inputs to coastal waters (https://data.gcoos.org/), which makes it an ideal region to test the integration of nutrient sensors into existing programs.

A wet chemical nitrate sensor (WIZ probe, SYSTEA S.p.A., Anagni, Italy) was deployed at the Sanibel-Captiva Conservation Foundation (SCCF) River, Estuary and Coastal Observing Network (RECON) Shell Point monitoring platform (26.5226, − 82.0080) at the mouth of the Caloosahatchee River (Fig. 1) for approximately 1 year, from 01 March 2020 through 16 February 2021 (353 total days, Table 1). Established in 2007, the RECON monitors water quality including salinity, water temperature, fluorescent dissolved organic matter (fDOM), dissolved oxygen (mg L^{-1} and % saturation), sensor depth, turbidity, chlorophyll-*a* (chl-a), and flow velocity. There are six sites within the Caloosahatchee River and Estuary (http://recon.sccf.org/sites/shell-point/about) out to the GoM. The RECON Shell Point location in the lower estuary where phytoplankton are thought to be nitrogen-limited for most of the year (Garcia et al., 2015; Heil et al., 2007). The estuary experiences semidiurnal tides that averaged 0.6 m over the study period. The site is also downstream of an urbanized tidal watershed with over 600 km of canals and largely residential land use that is under the Caloosahatchee Estuary Watershed Basin Management Action Plan (BMAP) which sets total maximum daily loads for total nitrogen (FLDEP, 2012). Enhanced nitrate monitoring is therefore of great importance in this system

Another WIZ probe was deployed at the Louisiana Universities Marine Consortium (LUMCON) DeFelice Marine Center monitoring station (29.2550, − 90.6664; Fig. 1) from 12 March 2020 to 26 October 2020 (228 total days, Table 1). Similar to SCCF, the intention was to deploy the WIZ for 1 year, but Hurricane Zeta made landfall in Louisiana (27–29 October 2020) causing substantial damage to the dock at which the WIZ was deployed, thus delaying the redeployment of the sensor.

At the northern boundary of Terrebonne Bay, the deployment site is set within a diurnal, microtidal salt marsh ecosystem with *Spartina alterniflora* dominating the marsh (Hill and Roberts, 2017) and inundation more often driven by wind than tides (Turner,

Table 1
Deployment details for both deployment types. Asterisks indicate sample size for reference samples taken at the surface.

Deployment type	Site	Location	Deployment period	Total days	Days of sensor data	Total intake reference samples	Matched reference samples
Self-Contained	SCCF	26.5226, − 82.0080	03/01/2020–02/16/2021	353	161	10	9
Fully Integrated	LUMCON	29.2550, − 90.6664	03/12/2020–10/26/2020	228	26	33 (32*)	5 (5*)

2001). Tidal heights range from − 1.05 m to 0.41 with a mean range of 0.31 m (NOAA Station 8762928, approximately 1 km from the deployment site) and mean depth at the deployment site of approximately 1.8 m. The Louisiana coastal marshes receive freshwater from the Mississippi and Atchafalaya Rivers which increases nutrient inputs to these ecosystems, mainly from upstream fertilizer use (Parsons et al., 2006). The monitoring station at the LUMCON Marine Center provides continuous water quality data including water temperature, water height, specific conductivity and salinity, dissolved oxygen (mg L^{-1} and % saturation), and chl-a (http://weatherstations.lumcon.edu/index.html).

2.2. Sensor details

The WIZ has been on the commercial market since 2009 (Moscetta et al., 2009), and could be considered to have achieved TRL 8. It has proven to be competitive in nutrient sensing as hundreds of units have been sold worldwide (e.g., Bodini et al., 2015; Vuillemin et al., 2009). The sensor consists of an upper reagent canister with reagent bags that connect to the hydraulic circuit, and a lower analytical unit (Fig. 2) that houses the micro-Loop Flow Reactor (μLFR) including all mechanical, hydraulic, and optical devices, as well as the heating and UV units (Copetti et al., 2014). The 4 mL hydraulic circuit is controlled by a peristaltic pump that collects samples, introduces reagents from the reagent canister, and mixes the liquids. The optical detectors include a 20 mm spectrophotometric flow-cell and a 10 mm quartz fluorometric flow-cell. In laboratory preparation and field deployment, the hydraulic circuit also has lines specific for normal waste, toxic waste, and Milli-Q that is used in washing the system between analyses. When deployed in the field, the normal waste line is free within the water column while the toxic waste line attaches to an external 5 L bag (Fig. 2). The Milli-Q line leads to an external 5 L bag filled with 3.5 L of Milli-Q water (Fig. 2).

The sensor has a nitrate method detection limit (MDL) of 0.05 μM (Johengen et al., 2017c) and employs the VCl_3 reduction method. First, a VCl_3 + HCl solution is added to the water sample to reduce nitrate to nitrite. The Griess reagent, sulfanilamide (SAA) and *N*-(1-Naphthyl)ethylenediamine dihydrochloride (NED), is then added to the reduced nitrate plus nitrite causing a reaction that results in a pink azo dye measured at 525 nm (Zhang and Wu, 1986) by the internal spectrophotometer. The sensor provides a single datapoint of nitrate concentration for each sampling event. A double range VCl_3-NO_3^- special calibration procedure was performed to calibrate the sensor for the nitrate method.

2.3. Deployment details

Sensors were deployed at the two sites in different ways: as a self-contained unit at SCCF and integrated into a larger monitoring

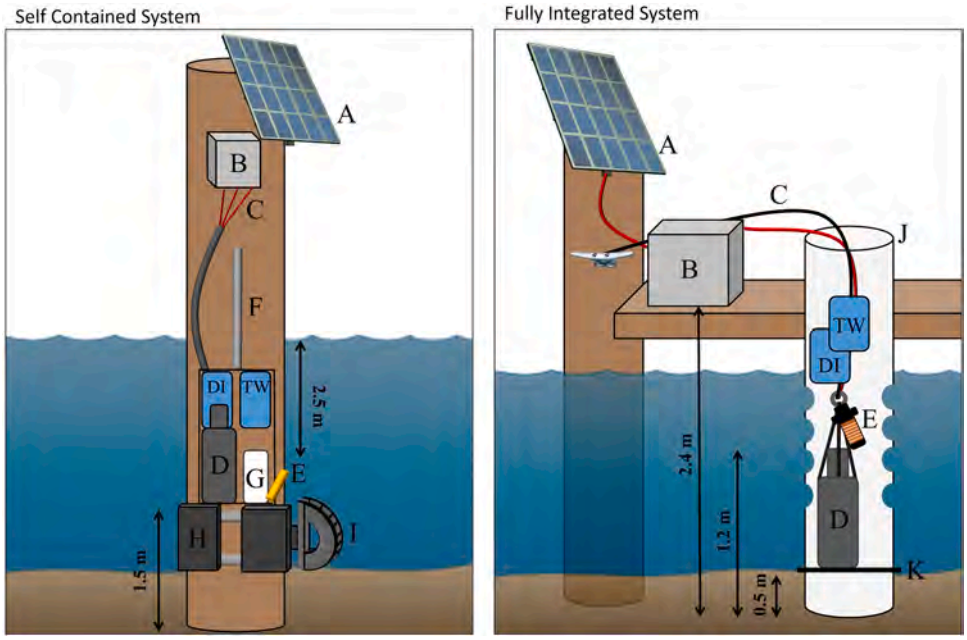

Fig. 2. Schematics representing deployment configurations – self-contained (left) and fully integrated (right). Both units were powered by solar panels (A) and a battery enclosed in a junction box with a datalogger and other power components (B). Power and communication cables (C) ran from the sensor (D) to the electronics box (B). Each sensor had an intake unit (E) that included filters (left: 0.1 μm; right: 25 μm). The self-contained unit (left) was deployed using an aluminum pipe (F) and was attached to the mooring frame that housed (D), the pump (G), DI water (DI) and toxic waste (TW) bags. The mooring frame rested on the RECON support structure (H) that also held the RECON water quality sensors (I). The fully integrated unit (right) utilized a PVC pipe (25.4 cm) with holes which allowed water flow through. The sensor rested on a large bolt (K) to ensure the sensors remained 0.5 m above the sediment.

platform at LUMCON (Fig. 1). The self-contained system utilized components supplied by the manufacturer (SYSTEA S.p.A) including datalogger and pump. The fully integrated system used non-Systea equipment, including a commercially available, widely used datalogger (CR1000, Campbell Scientific, Inc., Logan, Utah, United States).

2.3.1. Self-contained system (0.1 μm pre-filter)

The self-contained system was equipped with a 0.1 μm filtration unit at the intake, including a copper pre-filter, and hollow fiber filtration cartridge, peristaltic pump (to operate the filter), and a three-way valve to perform sampling and backflushing (Table 2; Fig. 2, left panel). A manufacturer-provided datalogger (ZetaLOG, SYSTEA S.p.A.) was used to perform sensor operation and provide data in real-time via cellular telemetry. The datalogger also provided the ability to conduct daily internal calibrations, but due to manufacturer suggestion the internal calibrations were used only as a reference point, not to automatically update calibrations. The sensor was powered by a 12 V, 31.6 A h rechargeable battery connected to a 12 V charge controller (Sunsaver, Morningstar Corporation, Newton, Pennsylvania, United States) and two 20 W monocrystalline solar panels.

The sensor was mounted on a piling separately from the co-located RECON water quality sensors and was attached to the end of a 1" aluminum pipe (Table 2; Fig. 2, left panel). To address biofouling, the entire deployment cage was wrapped with black stretch wrap (Table 2; Fig. A.1A). The copper sample intake was attached to the cage outside the wrap and the sensor intake was placed 2.5 m below the water surface (approximately 1.5 m from the sediment surface). The sensor was calibrated prior to deployment and every 30 days thereafter using the double range VCl_3-NO_3^- calibration procedure, according to manufacturer's recommendation. The used reagent canister was swapped with a second, filled reagent canister every 30 days. Samples were collected once every 2 h during deployment.

To facilitate quantification of sensor performance at this site, discrete reference samples were collected monthly near the sensor intake (approximately 2 m depth) using a Van Dorn water sample. Reference samples were filtered through a 0.45 μm syringe filter and frozen at − 20 °C before being analyzed at SCCF for $NO_3^- + NO_2^-$ using an autoanalyzer (AutoAnalyzer 3, SEAL Analytical, Incorporated, Mequon, Wisconsin, United States) using standard methods (EPA 353.2). Salinity, temperature, and chl-a were collected every 1 h from 01 March 2020 to 16 February 2021 (Fig. 3) using a Seabird WQM (Sea-bird Scientific, Bellevue, WA, United States). A Seabird ECO (Sea-bird Scientific) was used to measure fDOM at the Shell Point RECON station. Turbidity was measured using an optical sensor included in the WQM and, at times, was susceptible to biofilm growth which may have caused interference. Turbidity datapoints that sharply increased well above previous and subsequent datapoints were considered outliers and were removed from the dataset. A known malfunction of the chl-*a* sensor caused abnormally high readings (up to 73.0 μg L^{-1}) during March and April 2020; therefore, readings > 10 μg L^{-1} were removed from this study.

2.3.2. Fully integrated system (25 μm pre-filter)

The fully integrated sensor was equipped with a 25 μm filter at the intake and controlled by a commercially available datalogger (CR1000) outfitted with a solid-state relay (Sensata-Crydom, Crydom, San Diego, California, United States; Table 2; Fig. 2, right panel). The sensor was powered by a 12 V 50 Ah rechargeable battery connected to a 70 W monocrystalline solar panel and a 3 A solar panel voltage regulator (High Sierra Electronics, Inc., Grass Valley, California, United States). Biofouling was mitigated using copper tape (Table 2; Fig. A.1B) due to the smaller formfactor of the sensor. The sensor was deployed in a dock-mounted PVC pipe (25.4 cm diameter) that was driven into the sediment. Sensor sampling frequency was set to 2 h. The program used for the datalogger did not allow for wash cycles between samples, nor internal calibrations. The reagent canister was swapped with a second, filled reagent canister each time the sensor was redeployed. Since the sensor was deployed for shorter periods of time at this site, calibration using the double range VCl_3-NO_3^- calibration procedure, according to manufacturer's recommendation only occurred prior to the first deployment.

Reference samples were collected weekly at two depths: 0.5 m below the air-water interface and approximately 1.2 m above the sediment surface, the same depth as the sensor intake. Samples were filtered through a sterile 0.22 μm PES syringe filter (Simsii, Inc., Issaquah, WA, United States) and stored frozen before analysis for $NO_3^- + NO_2^-$ at the LUMCON Ecosystem Ecology and Biogeochemistry Lab using the VCl_3 method (Schnetger and Lehners, 2014) on an BioTek Epoch 2 microplate reader. Standard curves (R^2 values ≥ 0.99) were prepared by diluting NO_3-N and NO_2-N stock solutions (Hach Company, Loveland, CO, United States). For the purposes of this study, salinity, temperature, and chl-*a* data were collected every 15 min using an EXO2 sonde (YSI Incorporated, Yellow Springs, Ohio, United States) from 12 March to 26 October 2020 (Fig. 4). The EXO2 sonde was mounted at the same deployment site as the nutrient sensor and taken offline during Hurricanes Laura (20–29 August 2020), Beta (17–25 September 2020),

Table 2
Different components included in the two deployment configurations, Self-Contained and Fully Integrated.

	Self-Contained (SCCF)	Fully Integrated (LUMCON)
Sensor sampling depth	2.5 m	1.2 m[¥]
Reference sampling depth	2 m	0.5 m, 1.2 m[¥]
Intake filter pore size	0.1 μm	25 μm
Reference filter size & type	0.45 μm nylon syringe filter	0.22 μm PES syringe filter
Automatic backwash pump	Yes	No
Datalogger	Zetalog (SYSTEA S.p.A.)	CR1000 (Campbell Scientific)
Fully functional program	Yes	Lacked backwash function, internal calibration, cleaning cycles
Antibiofouling Method	Enclosed in plastic bag	Copper tape

[¥] Distance above the sediment surface.

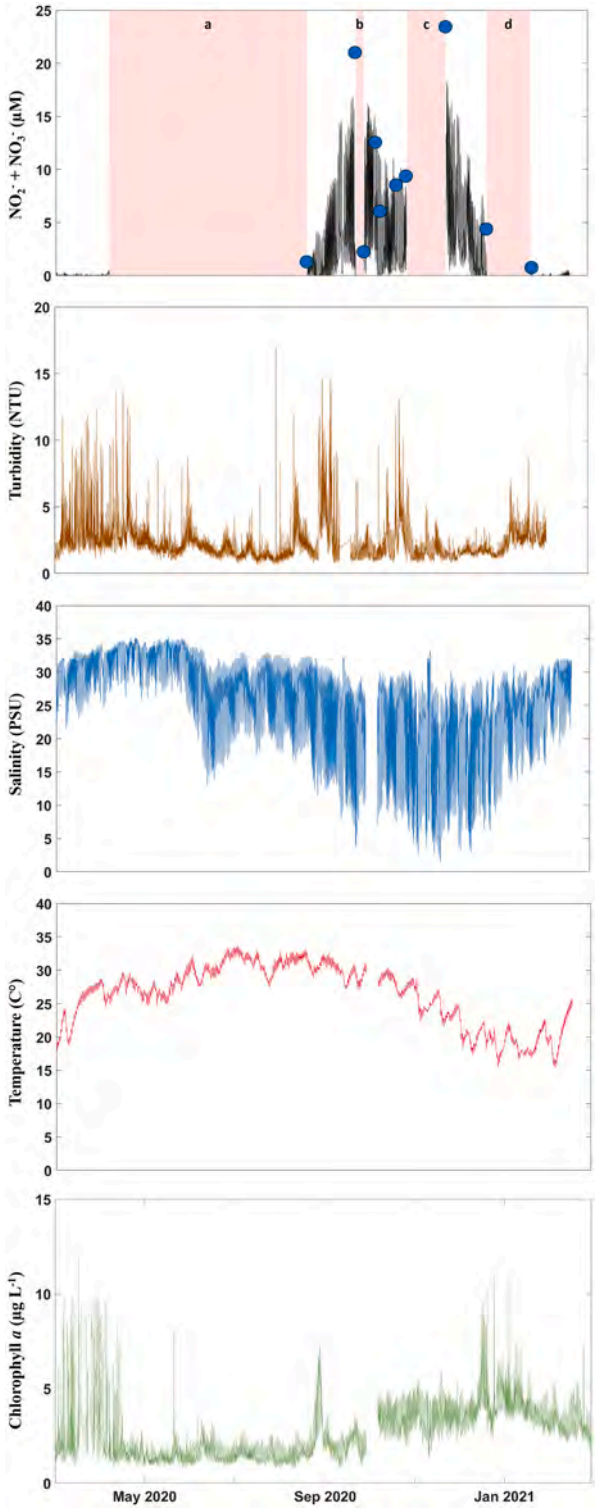

Fig. 3. Water quality measurements taken at the SCCF deployment site including sensor nitrite + nitrate (black line), intake-depth reference nitrite + nitrate (blue circles), turbidity (brown line), salinity (blue line), temperature (red line), and chlorophyll-*a* (green line). Red blocks indicate times in which the sensor was not deployed due to a) COVID-19 lockdown protocols, b) sensor maintenance, c) sensor troubleshooting, d) nitrate being below the limit of detection in the dry season. Negative sensor-based nitrite + nitrate measurements were removed.

and Delta (4–11 October 2020). Continuous turbidity data is not collected at this site, but discrete TSS samples and TDS using a YSI Pro30 meter (YSI Incorporated) were recorded.

2.4. Statistical analyses

The purpose of this study was to assess variables affecting integration of commercially available, wet chemical nitrate sensors into existing estuarine monitoring efforts. Past studies have conducted in-depth verification tests of WIZ sensor performance against reference samples across a range of conditions (Bodini et al., 2015; Copetti et al., 2017; Johengen et al., 2017c; Wild-Allen and Rayner, 2014). As a result of this available data and differences in deployment and site in the current study, statistical analyses of the sensor and reference data have been kept to a minimum. Spearman's rank correlation (Spearman, 1904) was carried out to evaluate relationships between sensor-measured nitrate and other water quality variables (salinity, temperature, chl-*a*, and turbidity, when available) for each site. Correlation coefficients range from − 1 to 1 with values closer to − 1 or 1 indicating strong negative or positive linear relationships, respectively, and coefficients near zero indicating a weak relationship. For these analyses, concentrations below the

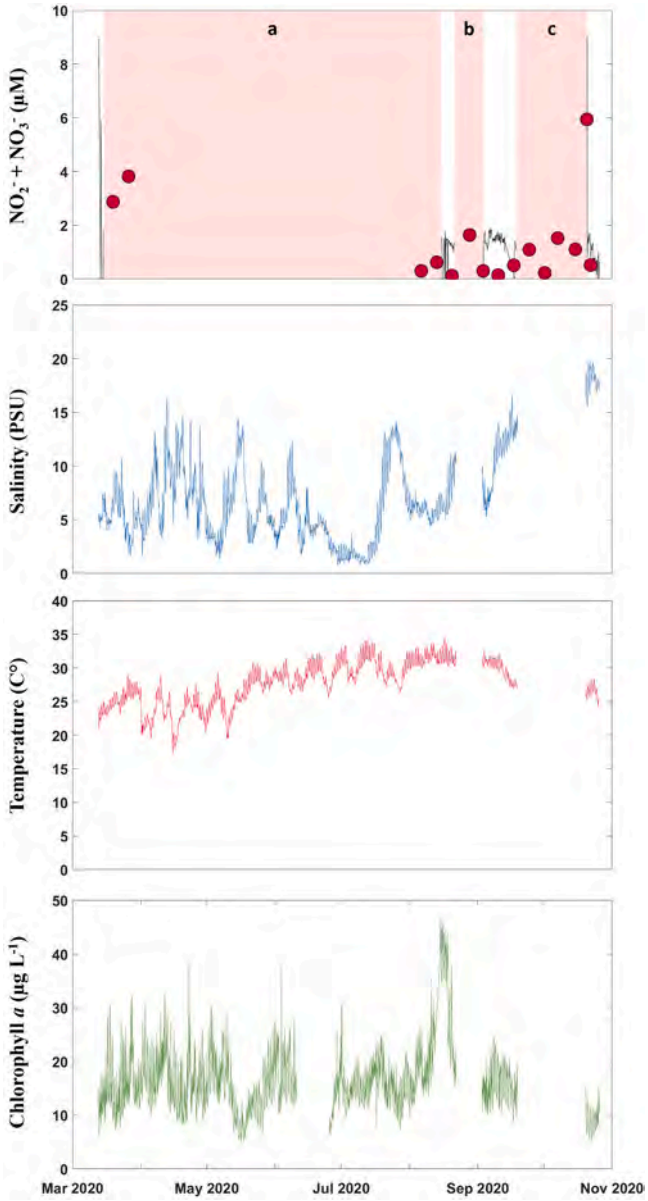

Fig. 4. Water quality measurements taken at the LUMCON deployment site including sensor nitrite + nitrate (black line), intake-depth reference nitrite + nitrate (red circles), salinity (blue line), temperature (red line), and chlorophyll-*a* (green line). Red blocks indicate times in which the sensor was not deployed due to a) COVID-19 lockdown protocols, b) Hurricane Laura, and c) Hurricanes Beta and Delta.

method detection limit (< MDL) were removed (self-contained unit, n = 1029; fully integrated unit, n = 260 [< MDL and negative values removed]). To conservatively compare sensor- and reference-derived nitrate data, sensor datapoints measured within 3 hours of the reference samples were averaged and visually compared using correspondence plots with a 1:1 line to identify sensor under- (datapoints below the 1:1 line) or overestimation (datapoints above the line) of nitrate. The 3-hour range for matched data was selected to ensure we had at least two sensor data points to average and match the reference sample while also ensuring data from both methods were kept as close in time as possible. No statistical analyses were performed on matched data because of the low sample sizes (self-contained unit, n = 9; fully integrated unit, n = 5) and the availability of robust sensor verification data elsewhere (Johengen et al., 2017c). All statistical analyses were performed in MATLAB (Mathworks, R2022a).

3. Results

3.1. Deployment duration and sensor performance

During the deployment period of the self-contained unit (0.1 μm pre-filter), a total of 161 days of continuous data and 10 discrete reference samples were collected. The sensor was not deployed for 192 days within that period (Table 1) due to COVID-19 lockdown protocols (127 days) and maintenance (34 days). The sensor was also taken offline for 31 days (Fig. 3) during the dry season when nitrate was < MDL. Generally, concentrations of nitrate were higher in the discrete samples (mean: 8.94 μM) than those measured by the sensor (mean: 4.19 μM). Sensor-measured nitrate concentrations for the full deployment period ranged from 0.071 μM to 18.3 μM on 24 November 2020. Discrete reference samples ranged from 0.73 μM to 23.4 μM (Fig. 3; Table 3).

During the deployment period of the fully integrated system (25 μm pre-filter), the sensor collected 26 days of data with gaps due to COVID-19 lockdown protocols (155 days) and Hurricanes Laura, Beta, and Delta (47 days; Fig. 4; Table 1). During sensor deployment, a total of 65 reference samples were collected, but only 10 fell on the same day as sensor measurements (Table 1) and only 5 reference samples at each depth matched the sensor data (i.e., within 2 h; Table 1). Sensor-measured nitrate concentrations ranged from < MDL to 9.07 μM (mean = 1.47 μM [< MDL removed]). Nitrate concentrations from the 65 reference samples across the entire deployment period ranged from 0.070 to 12.9 μM at the surface and 0.060 to 12.5 μM at the intake depth with means of 2.94 μM (surface) and 2.81 μM (intake; Fig. 4; Table 3), suggesting similar concentrations between the two depths and a mixed water column. It should be noted that nitrate concentrations at this site (LUMCON) tend to be seasonally varying, with low concentrations occurring during summer and fall (June–November) and higher and more variable during winter and spring (December–May; Fig. A.2).

The small number of matched sensor- and reference-derived nitrate datapoints (n = 5 or 9, depending on site) limits our ability to make significant insights into sensor performance. Additionally, the purpose of this study was to more fully assess the factors influencing integration of these sensors into existing monitoring programs. Nonetheless, the two deployments of the same sensor technology indicate some notable differences in relationships between sensor- and reference sample-derived nitrate concentrations. The self-contained deployment showed a positive trend between sensor and reference nitrate concentrations (linear regression, $p = 0.103$, adjusted $R^2 = 0.239$, n = 9) and across a large range in concentrations (up to nearly 25 μM). Generally, the sensor underreported nitrate relative to reference samples in datapoints where both were available (89 %; Fig. 5A). The fully integrated deployment experienced a much smaller range of nitrate concentrations (< 1 μM) where matched sensor and reference data were available. Likely as a result, sensor- and reference-derived data were not well correlated at either depth of sampling for this deployment (Surface: Fig. 5B, Intake: Fig. 5C). The water column was mixed at the time of sampling, therefore both sampling depths were the same water mass being compared. These differences in nitrate at the two sites are emphasized by sensor and reference comparisons over smaller temporal scales (Fig. 6). Over 8-day periods in September-October 2020, the self-contained unit measured nitrate ranging from

Table 3
Environmental conditions for the Self-Contained and Fully integrated deployments at SCCF and LUMCON, respectively. Sensor-based nitrate concentrations that were below the method detection limit (0.05 μM) are indicated as "< MDL" and were not used in the calculation of mean concentrations.

Parameter	Minimum	Maximum	Mean
Self-Contained (SCCF)			
Sensor nitrate (μM)	< MDL	18.3	4.19
Intake reference nitrate (μM)	0.73	23.4	8.94
Salinity (PSU)	1.44	35.2	25.2
Temperature (°C)	15.4	33.6	26.1
Chlorophyll-*a* (μg/L)	0.730	18.0	2.67
Turbidity (NTU)	0.650	17.0	2.36
Fully integrated (LUMCON)			
Sensor nitrate (μM)	< MDL	9.07	1.47
Intake reference nitrate (μM)[¥]	0.06	12.5	2.54
Surface reference nitrate (μM)[**]	0.07	14.01	3.48
Salinity (PSU)	0.790	19.7	6.89
Temperature (°C)	17.2	34.5	27.6
Chlorophyll-*a* (μg/L)	5.00	46.7	16.2

[¥] Reference samples at the sensor intake (1.2 m) during the period 19 March–30 December 2020.
[**] Reference samples below air/water interface (0.5 m) during the period of 2 January–30 December 2020.

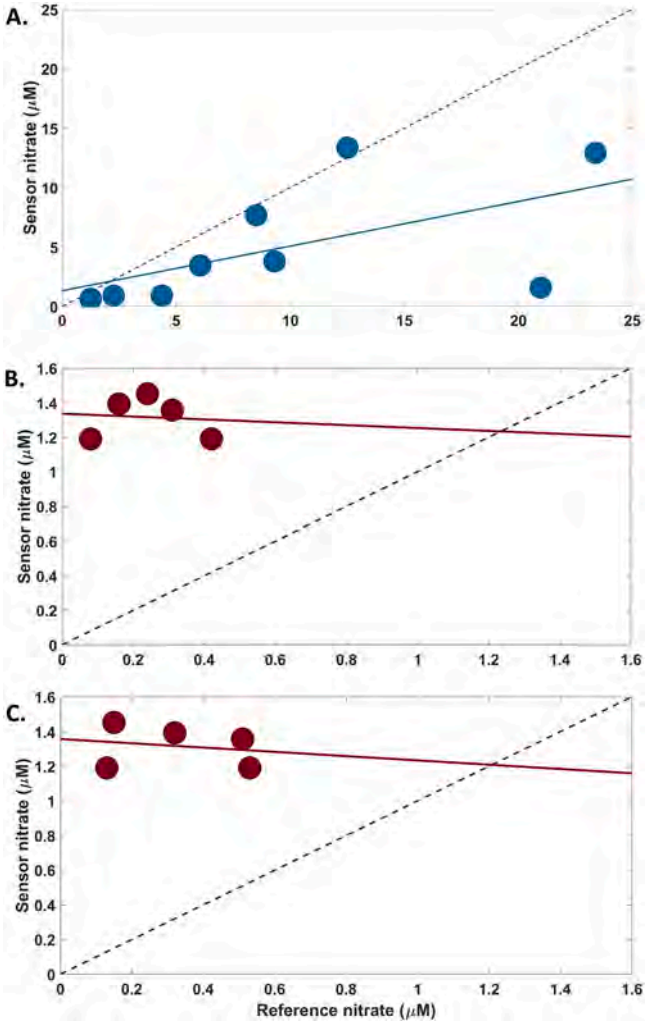

Fig. 5. Correspondence plot of sensor- versus reference-measured nitrate for the a) self-contained unit, and the fully integrated unit when compared to reference samples taken at the b) surface of the water column and c) same depth as the sensor intake. Blue (self-contained unit) and red (fully integrated unit) dots are matched observations within 3-h of each other. All negative and < MDL values were removed. Dashed line represents a 1:1 correspondence and the blue (self-contained unit) and red (fully integrated unit) lines denote the linear regression.

0.214 μM to 10.1 μM (mean= 4.01 μM), with diel or tidally-driven patterns of nitrate fluctuation and generally good agreement with reference samples (n=2; Fig. 6A). During this shorter timeframe, the fully integrated unit measured nitrate ranging from 1.07 μM to 1.86 μM (mean = 1.51 μM), higher than reference samples during the 8-day period (0.15–0.32 μM; Fig. 6B) and consistent with the longer dataset.

3.2. Other environmental data

Turbidity at SCCF Shell Point (self-contained unit), located within the Caloosahatchee River Estuary, varied over a wide range (0.650–17.0 NTU, excluding outliers [see Methods]) with mean turbidity of 2.36 NTU (Table 3). Salinity (mean: 25.2 PSU) and water temperature (mean: 26.1°C) showed diurnal patterns and ranged from 1.44 to 35.2 PSU and 15.4 to 33.6 °C (Table 3), respectively. SCCF Shell Point chl-*a* (mean: 2.67 μg l^{-1}) ranged from 0.730 to 18.0 μg l^{-1} (Table 3). Nitrate (mean: 4.19 μM) ranged from < MDL – 18.3 μM and a diurnal pattern was observed with high concentrations typically occurring mid to late day (Fig. 6A). Spearman's rank correlation revealed that sensor-measured nitrate (μM) was significantly ($p \leq 0.05$) correlated to all other environmental variables (turbidity, $p < 0.001$; salinity, $p < 0.001$; temperature, $p = 0.19$; chl-*a*, $p < 0.001$). The strongest correlation was between salinity and nitrate in a negative direction ($r_s = -0.85$). All other environmental parameters had weaker, positive relationships with nitrate (turbidity, $r_s = 0.28$; temperature, $r_s = 0.04$; chl-*a*, $r_s = 0.32$).

LUMCON experienced a narrower range of temperature (17.2–34.5 C°, mean: 27.6 °C) and salinity (0.790–19.7 PSU, mean: 6.89 PSU) but a wider range of chl-*a* (5.00–46.7 μg l^{-1}, mean: 16.2 μg l^{-1}; Table 3). Sensor-measured nitrate (mean: 1.47 μM) did not vary

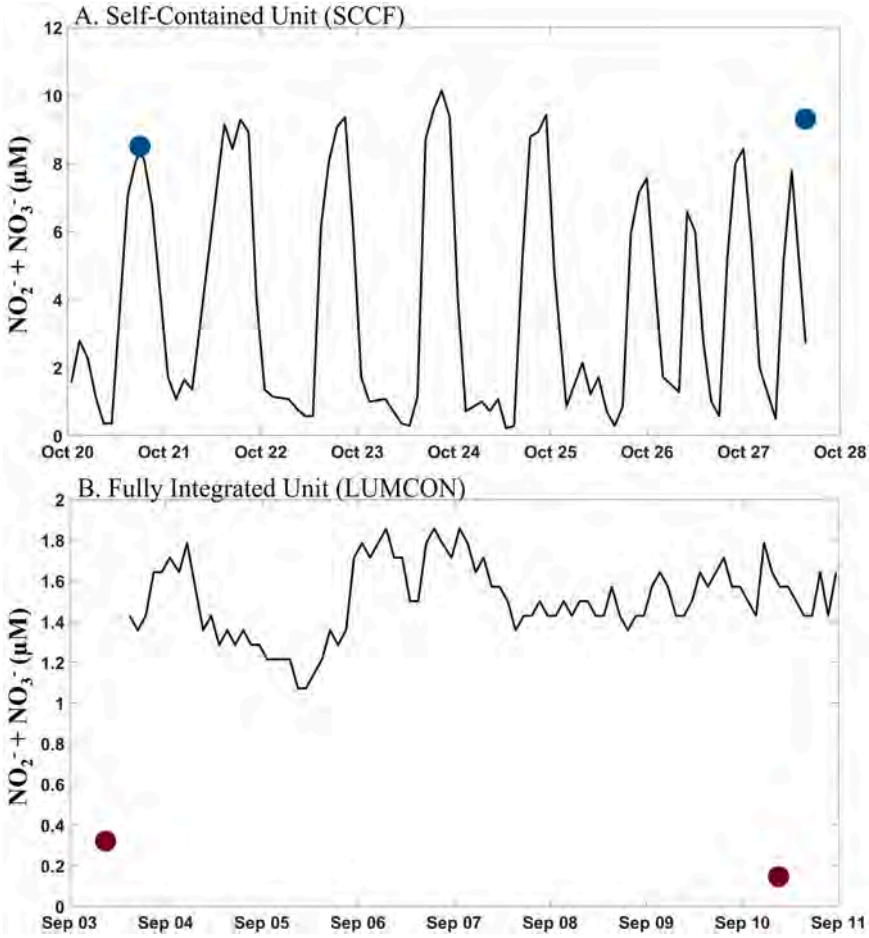

Fig. 6. Nitrate measurements over 8-day periods for the self-contained unit (A) and the fully integrated unit (B). Fully Integrated unit only includes intake-depth (1.2 m above sediment) reference samples.

much throughout the deployment period, ranging from < MDL – 9.07 µM. Nitrate was significantly ($p < 0.001$) correlated with salinity ($r_s = -0.38$), temperature ($r_s = 0.32$,) and chl-*a* ($r_s = 0.24$).

4. Discussion

The current study addresses integration of newer, commercially available nutrient sensor technologies into real-world monitoring systems. The study also seeks to provide insights into sensor performance at different estuarine sites and considers best practices for integrating continuous nutrient monitoring into existing programs and platforms. The study was not designed to provide exhaustive sensor performance verification testing, as those tests for the sensor used in this study (Copetti et al., 2017; Johengen et al., 2017c) and others (Grand et al., 2017; Johengen et al., 2017a, 2017b; O'Boyle, Partington, 2014; Rieger et al., 2008) have already been done and are available to potential adopters. The WIZ sensor has proven to be a valuable tool in providing reliable real-time, high-frequency nutrient data, especially when deployed in the self-contained configuration. Although issues arose with the fully integrated configuration, progress towards integrating the WIZ into current monitoring programs may be achieved with a few improvements.

4.1. *In situ* sensor performance

Sensor performance (evaluated as comparisons to reference samples) differed between the two sites and deployment types in this study, with the self-contained unit equipped with 0.1 µm pre-filter typically underestimating and the fully integrated unit equipped with 25 µm pre-filter typically overestimating nitrate concentrations. However, the nutrient concentrations for the two environments cannot be directly compared, as the maximum concentrations measured by the fully integrated unit at LUMCON (1.47 µM) were below the average concentration measured by the self-contained unit at SCCF (4.19 µM). It is likely that observed differences in sensor performance relative to reference samples were related to where in the dynamic range of the sensor it was being operated. A prior study evaluating the performance on the WIZ nutrient sensor showed poor linearity at low NO_3 concentrations (0–0.05 mg N l^{-1}; (Johengen

et al., 2017c)). During the duration of the study, samples from LUMCON occurred during the time of year when concentrations are their lowest for the year (June–November; Fig. A.1A and A.1B). These limitations of dynamic range suggest that detection at the low concentrations experienced by the fully integrated unit at LUMCON may contribute to poor sensor performance, and quantifying low concentrations with this sensor still represents a challenge.

An additional mechanism explaining the poor correlation between sensor and reference sample concentrations may also be the small number of samples for the fully integrated unit where both datapoints were available (n = 5). This was largely a function of pandemic and hurricane-related interruptions in deployments. Future deployments may consider adding more reference sample collection events when the sensor is deployed to better quantify sensor performance and deploying the sensor for increased duration to capture high and low concentration periods of the year.

Differences in sensor intake pre-filter and reference sample filter pore sizes may also explain some of the disagreement between the sensor v. reference concentrations in the two deployments. The self-contained unit had an intake pre-sensor filter size of 0.1 μm with discrete reference samples filtered with a 0.45 μm filter. The fully integrated sensor used a 25 μm pre-filter at the intake and reference samples were filtered with a 0.22 μm filter. This two orders or magnitude difference in filter sizes likely led to the fully-integrated sensor deployed at LUMCON capturing more particulate nitrogen (i.e., those bound to sediment particles and/or within phytoplankton cells) which was excluded by the smaller pore-sized filter used to collect reference samples. Water quality data collected alongside the nitrate sensor deployments may provide support for this mechanism, as an increase in chl-*a* (a proxy for phytoplankton biomass) in August 2020 at the LUMCON site (Fig. 4) occurred with observed overestimation of nitrate concentrations (Fig. 5B–C). Thus, it is likely that mismatch in sensor and reference sample filter pore sizes explain at least some of the disagreement in sensor v. reference concentrations in the fully integrated unit.

A mismatch in filter sizes may also explain the trend of underestimation of nitrate concentrations by the self-contained unit at SCCF. Here, the sensor intake pre-filter (0.1 μm) was smaller than the discrete reference sample filter (0.45 μm), which may have led to relatively more particulate nitrogen being measured in the reference samples than by the sensor. The use of a 0.45 μm filter may also allow inorganic nanoparticles of various minerals into the sample leading to the overestimation of dissolved nutrients (River and Richardson, 2019), although it is generally considered sufficient for and widely used in dissolved nutrient sample filtration (Reed et al., 2022).

4.2. Limitations to deployment

Duration of deployment was a primary difference between the two sites, but one that was seemingly unrelated to the sensors themselves. The self-contained unit collected 161 days of data (out of 353 total) and the fully integrated unit collected data for 26 (out of 228 days), largely as a result of the effects of the COVID-19 pandemic and limited access to deployment sites, tropical storms and hurricanes (especially at LUMCON) and the requirements for calibration, maintenance, and troubleshooting. Deployment duration of the integrated system was additionally impacted by storm surge flooding of the dock on which the sensor was deployed. Relocation of the sensor electronics to a nearby tower (where the water quality station is mounted, exclusive of the nutrient sensor) was attempted but the standard cable (5 m) was too short to reach the tower and a longer cable (15 m) suffered communication issues. As a result, the sensor electronics remained on the dock but were removed during storms leading to 44 days of missing nutrient sensor data (Fig. 4). These limitations in deployment duration led to small sample sizes for matched observations at both sites and especially for the fully integrated deployment (n = 5). All the matched observations at the fully integrated site fell at reference nitrate concentrations $<$ 0.5 μM, and this limited sample size and range of concentrations at the lower end of the limit of detection (see above) likely contributed to the poor comparisons between the sensor- and reference methods.

However, even with the shorter deployment periods, the sensors were able to capture temporal trends in nitrate concentrations that otherwise would have been missed with discrete reference samples. For example, nitrate concentrations in the lower Caloosahatchee River estuary (self-contained unit) showed clear diurnal fluctuations (Fig. 6A), likely due to the assimilation of nitrate by phytoplankton during daylight hours (e.g., Bates, 1976; Cochlan et al., 1991) and/or tidally mediated transport of nitrate – known to help fuel HABs in the region – into the estuary from the urbanized watershed (Gilbert et al., 2019; Ma et al., 2020; Medina et al., 2022). These data-driven insights are important since discrete samples for nutrients at this site are typically taken monthly, a sampling frequency that limits our abilities to resolve such diel fluctuations in nitrate. While sensor-measured nitrate concentrations in the upper reaches of Terrebonne Bay (fully integrated unit) varied less widely across the shorter, 8-day period in September 2020 (Fig. 6B), fluctuations within and between days add important detail to the expectation that nutrient dynamics in this system are seasonal (Fig. A.2) or event-related.

4.3. Sensor integration

The two sensor units differed in how they were deployed. Use of the manufacturer-supplied datalogger to remotely control the sensor in the self-contained unit allowed for the sensor to perform backwash cycles between samples. The utility of built-in telemetry to transmit data in real-time also helped troubleshoot sensor issues remotely and adjust (trigger, disable) on-demand sampling via text messaging. In contrast, the fully integrated sensor deployment utilized a commercially-available datalogger that was limited in its functionality due to lack of SDI-12 protocol, a serial communication protocol regularly included as an option for commercial environmental sensors (Cario et al., 2017; O'Boyle, Partington, 2014; Poornima et al., 2016; Snazelle, 2015a, b). A custom CRBasic program allowed datalogger access to basic sensor operations, i.e., turning the sensor on, collecting and analyzing a water sample, and turning the sensor off. The custom program is available on GitHub (https://github.com/jenraabe/GoM-Nutrient-Sensor). Additional

functionalities such as internal calibrations and wash cycles were not available with the RS-232 protocol that was developed due to a combination of time limitations and availability of coding support. Thus, addressing the challenges of integrating the WIZ with a commercial datalogger (i.e., addition of SDI-12 protocol or a fully functional program for RS-232 protocol) should be prioritized for this sensor and others entering the marketplace.

Biofouling was a concern at both sites and approaches for mitigation slightly differed. It should be noted that both wet chemical and optical nutrient sensors must deal with biofouling as it can impact material entering the sensor and optical services, respectively. The additional hardware and larger deployment cage for the self-contained system created a larger surface area and greater potential for external fouling issues than the fully integrated unit. Copper tape could not be used due to the complex shape of the unit and the tubing connecting the sensor to the outer waste and water bags was too delicate. The self-contained unit was wrapped in plastic and kept in place using Gorilla tape (Fig. A.1A). This method worked well at preventing fouling; however, it required the sensor to be brought back to the lab to reapply the wrap each time the reagents were changed (approximately monthly). Since the fully integrated unit had a smaller form factor, copper tape was utilized (Fig. A.1B) and was effective in preventing biofouling for several months at a time. With these anti-fouling measures, neither site reported degradation of data due to biofouling.

4.4. Recommendations for future use and continued technology development

Deployment of the two sensor configurations in this study highlights the trade-offs with integration into existing monitoring programs. Deployment as a self-contained system had advantages related to full functionality of datalogger program control and real-time access to data but came with additional cost to add a secondary datalogger. Deployment of the sensor as a fully integrated system that utilized a commercial datalogger represented a more cost-effective model and one that leveraged existing community expertise in sensor control, but with trade-offs related to full sensor functionality.

Another important factor that impacts sensor performance and integration is selection of filter pore size for both the sensor and reference samples relative to the deployment environment and target analytes (i.e., dissolved v. particulate v. total N). Dissolved inorganic nutrients are recommended to be measured using filters with 0.22 or 0.45 μm pore size to best separate dissolved from particulate fractions (Reed et al., 2022), a method that is used in many estuarine monitoring protocols (NOAA, 2021; USEPA, 1993). In the ACT verification report, the manufacturer recommended different filter sizes and configurations depending on the type of environment (i.e., wastewater, low turbidity sea water, and highly turbid river water) which may help guide users on filter choice (Johengen et al., 2017c). However, use of an appropriate filter on the nutrient sensor is also related to the deployment configuration. The 25 μm sensor filter can be used with both the manufacturer-supplied and other commercial dataloggers. However, use of the 0.1 μm filter – which more closely matches pore sizes used for dissolved nutrient sampling – requires the manufacturer-supplied datalogger that can control the backwash pump function, critical to unclogging the filter. Ultimately, use of wet chemical nutrient sensors for determination of specific fractions of nitrate need better matching of sensor intake filter size with that predominantly used in collection of reference samples.

In summary, this study suggests that prospective users of newer nutrient sensors to the market should consider the following aspects in their decisions on sensor choice and integration into water quality monitoring programs:

a) Tradeoffs of integration in cost versus functionality – cost is considered affordable but integration with commercially available dataloggers needs custom programming for automated functions.
b) Matching sensor filter with reference sample filters – it is important that the selected sensor pre-filter size closely matches pore sizes used for reference samples as mismatching may lead to under- or overestimation of nutrient concentration.
c) Deployment site requirements – a 50–60 W solar panel and 45–60 Ah battery for power is needed. Increased space is needed for the self-contained system (0.5 m × 0.5 m × 1.25 m [L × W × H]) versus the fully integrated system. A minimum deployment depth of 765 mm (i.e., the height of the nutrient sensor body) is also required to ensure the unit remains fully submerged to help preserve reagents.
d) Access to analytical lab – preparation of reagents requires the use of a fume hood and storage space for reagents, and toxic waste holding and disposal is also needed. Validation of nutrient concentration requires analytical lab instrumentation.
e) Implement robust anti-fouling methods – the methods described in the current study (black stretch wrap, copper tape wrapping) represent approaches to preventing biofouling on a nutrient sensor with relatively large formfactor and external features. Individual anti-fouling solutions may vary, but this study provides two that were highly effective.

Continued development of continuous nutrient sensors should consider interoperability with commercially available dataloggers as an important element in transitioning these technologies to full operational status. Interoperability goals should include full sensor functioning with non-proprietary dataloggers, for example via implementation of SDI-12 communication protocols that would allow for full operation (i.e., wash cycles, internal calibration) that the RS-232 interface currently does not. Such protocols would also support better adherence to open data standards that are more commonly being required and adopted by funding agencies and organizations leading new sensor deployment (e.g., Grinspan and Worker, 2020; IOOS; Wilkinson et al., 2016; Willoughby, 2019). These advancements in communication protocols and interoperability would also facilitate both the cost- and space-efficiencies of integration and allow for real-time sensor control and monitoring. Integration with known technologies may also further expand the potential market of users. Together, users and developers of nutrient sensors can help build networks of high frequency nutrient data that are critical to addressing the persistent issues of nutrient pollution that affect coastlines around the world.

5. Conclusions

The study tested the operational status and integration of a commercial, in situ chemical analyzer for nitrate in two existing monitoring programs in Louisiana and Florida as a pilot study for the development of a nutrient monitoring program across Gulf of Mexico estuaries. Deployment configuration of the WIZ probe (self-contained versus fully integrated), alongside challenges to continued deployment due to the COVID-19 pandemic and hurricane activity, seemed to affect agreement between the sensor- and reference sample-measured concentrations of nitrate. The results from this study support the need for sensor users to match filter sizes between instruments and reference samples. The temporally dense data that was collected shows promise for utility in efforts to understand and ultimately manage nitrogen in estuarine ecosystems. However, the limitations in functionality in the fully integrated unit suggests that incorporation of these sensors into existing monitoring assets is still a challenge. Better addressing interoperability of equipment among manufacturers will enhance the reach of newer technologies to help support expanded collection of continuous nitrate data throughout the Gulf of Mexico and beyond.

Funding

This research was supported by funding from National Oceanic and Atmospheric Administration (NOAA) via the Alliance for Coastal Technologies [Award NA16NOS0120017] and the Gulf of Mexico Coastal Ocean Observing System (GCOOS, [Awards NA16NOS0120018 and NA21NOS0120092]).

CRediT authorship contribution statement

Amanda Fontenot: Writing – review & editing, Investigation. **Sierra Greene:** Writing – review & editing, Investigation. **Jennifer Raabe:** Writing – original draft, Visualization, Investigation, Formal analysis. **Gulce Kurtay:** Writing – review & editing. **Brian J. Roberts:** Writing – review & editing, Supervision. **Beth A. Stauffer:** Writing – review & editing, Supervision, Conceptualization. **A.J. Martignette:** Writing – review & editing, Investigation. **Eric C. Milbrandt:** Writing – review & editing, Supervision.

Declaration of Competing Interest

The authors declare that they have no known competing financial interests or personal relationships that could have appeared to influence the work reported in this paper.

Data availability

Data will be made available on request.

Acknowledgements

We would like to thank collaborators at LUMCON, SCCF, Dauphin Island Sea Lab, University of Texas Marine Science Institute, U.S. Geological Survey (Tampa Bay), and Mote Marine Lab for their participation in technical workshops and for early troubleshooting of sensor use and deployments. Datalogger programming and technical assistance was provided by J. Adams and J. Davis at Campbell Scientific, Inc. Members of the Roberts lab at LUMCON (S. Plaisance, A. Davis) collected and analyzed LUMCON dock water samples for nitrate.

Appendix A. Supporting information

Supplementary data associated with this article can be found in the online version at doi:10.1016/j.eti.2024.103676.

References

Bates, S.S., 1976. Effects of light and ammonium on nitrate uptake by two species of estuarine phytoplankton. Limnol. Oceanogr. 21 (2), 212–218.

Bodini, S., Sanfilippo, L., Savino, E., Moscetta, P., 2015. Automated micro Loop Flow Reactor technology to measure nutrients in coastal water: state of the art and field application, OCEANS 2015 - Genova. Genova, Italy, pp. 1–7.

Breitburg, D., Levin, L.A., Oschlies, A., Grégoire, M., Chavez, F.P., Conley, D.J., Garçon, V., Gilbert, D., Gutiérrez, D., Isensee, K., Jacinto, G.S., Limburg, K.E., Montes, I., Naqvi, S.W.A., Pitcher, G.C., Rabalais, N.N., Roman, M.R., Rose, K.A., Seibel, B.A., Telszewski, M., Yasuhara, M., Zhang, J., 2018. Declining oxygen in the global ocean and coastal waters. Science 359 (6371).

Cario, G., Casavola, A., Gjanci, P., Lupia, M., Petrioli, C., Spaccini, D., 2017. Long lasting underwater wireless sensors network for water quality monitoring in fish farms, OCEANS 2017 - Aberdeen. pp. 1–6.

Cochlan, W.P., Harrison, P.J., Denman, K.L., 1991. Diel periodicity of nitrogen uptake by marine phytoplankton in nitrate-rich environments. Limnol. Oceanogr. 36 (8), 1689–1700.

Copetti, D., Valsecchi, L., Capodaglio, A.G., Tartari, G., 2017. Direct measurement of nutrient concentrations in freshwaters with a miniaturized analytical probe: evaluation and validation. Environ. Monit. Assess. 189 (4), 144.

Copetti, D., Valsecchi, L., Sanfilippo, L., Moscetta, P., Capodaglio, A., Tartari, G., 2014. Real-time evaluation of nutrient concentrations in surface waters using a portable probe. Systea S.p.a., Anagni, Italy.
Craig, J.K., 2012. Aggregation on the edge: effects of hypoxia avoidance on the spatial distribution of brown shrimp and demersal fishes in the Northern Gulf of Mexico. Mar. Ecol. Prog. Ser. 445, 75–95.
Craig, J.K., Crowder, L.B., Henwood, T.A., 2005. Spatial distribution of brown shrimp (Farfantepenaeus aztecus) on the northwestern Gulf of Mexico shelf: effects of abundance and hypoxia. Can. J. Fish. Aquat. Sci. 62 (6), 1295–1308.
Daniel, A., Laës-Huon, A., Barus, C., Blandfort, D., Guigues, N., Salter, I., Woodward, E.M.S., Beaton, A.D., Knockaert, M., Greenwood, N., Munaron, D., Achterberg, E. P., 2020. Toward a harmonization for using *in situ* nutrient sensors in the marine environment. Front. Mar. Sci. 6, 773.
FLDEP, Florida Department of Environmental Protection, 2012. Basin Management Action Plan for the Implementation of Total Maximum Daily Loads for Nutrients Adopted by the Florida Department of Environmental Protection in the Caloosahatchee Estuary Basin. Tallahassee, FL.
Garcia, J.C., Ketover, R.D., Loh, A.N., Parsons, M.L., Urakawa, H., 2015. Influence of freshwater discharge on the microbial degradation processes of dissolved organic nitrogen in a subtropical estuary. Antonie Van Leeuwenhoek 107 (2), 613–632.
Gilbert, M.H., Reidenbach, L.B., Milbrandt, E.C., Cramer, B.D., 2019. Nutrient analysis of the Caloosahatchee River and Estuary of southwest Florida. Geological Society of America. Geological Society of America.
Glibert, P.M., Beusen, A.H.W., Harrison, J.A., Durr, H.H., Bouwman, A.F., Laruelle, G.G., 2018. Changing land-, sea-, and airscapes: sources of nutrient pollution affecting habitat suitability for harmful alga. In: Glibert, P.M., Berdalet, E., Burford, M.A., Pitcher, G.C., Zhou, M. (Eds.), Global Ecology and Oceanography of Harmful Algal Blooms. Springer, Cham, pp. 55–76.
Grand, M.M., Clinton-Bailey, G.S., Beaton, A.D., Schaap, A.M., Johengen, T.H., Tamburri, M.N., Connelly, D.P., Mowlem, M.C., Achterberg, E.P., 2017. A lab-on-chip phosphate analyzer for long-term in situ monitoring at fixed observatories: optimization and performance evaluation in estuarine and oligotrophic coastal waters. Front. Mar. Sci. 4.
Grinspan, D., Worker, J., 2020. Implementing Open Data Strategies for Climate Action: Suggestions and Lessons Learned for Government and Civil Society Stakeholders: Working Paper. World Resources Institute, Washington, DC.
Hamilton, G., McVinish, R., Mengersen, K., 2009. Bayesian model averaging for harmful algae bloom prediction. Ecol. Appl. 19 (7), 1805–1814.
Harrison, P.J., Piontkovski, S., Al-Hashmi, K., 2017. Understanding how physical-biological coupling influences harmful algal blooms, low oxygen and fish kills in the Sea of Oman and the Western Arabian Sea. Mar. Pollut. Bull. 114 (1), 25–34.
Heil, C.A., Muni-Morgan, A.L., 2021. Florida's harmful algal bloom (HAB) problem: escalating risks to human, environmental and economic health with climate change. Front. Ecol. Evol. 9.
Heil, C.A., Revilla, M., Glibert, P.M., Murasko, S., 2007. Nutrient quality drives differential phytoplankton community composition on the southwest Florida shelf. Limnol. Oceanogr. 52 (3), 1067–1078.
Hill, T.D., Roberts, B.J., 2017. Effects of seasonality and environmental gradients on Spartina alterniflora allometry and primary production. Ecol. Evol. 7 (22), 9676–9688.
Howarth, R., Chan, F., Conley, D.J., Garnier, J., Doney, S.C., Marino, R., Billen, G., 2011. Coupled biogeochemical cycles: eutrophication and hypoxia in temperate estuaries and coastal marine ecosystems. Front. Ecol. Environ. 9 (1), 18–26.
The U.S. Integrated Ocean Observing System (IOOS), T.U.S.I.O.O.S., Data Portal. Silver Spring, MD.
Johengen, T., Purcell, H., Tamburri, M., Loewensteiner, D., Smith, G.J., Schar, D., McManus, M., Gordon Walker, Stauffer, B., 2017a. Performance verification statement for Real Tech Real Nitrate Analyzer GL Series. Alliance for Coastal Technology.
Johengen, T., Purcell, H., Tamburri, M., Loewensteiner, D., Smith, G.J., Schar, D., McManus, M., Walker, G., Stauffer, B., 2017b. Performance verification statement for NOC Nitrate Analyzer. Alliance for Coastal Technology.
Johengen, T., Purcell, H., Tamburri, M., Loewensteiner, D., Smith, G.J., Schar, D., McManus, M., Walker, G., Stauffer, B., 2017c. Performance Verification Statement for Systea Probe WIZ Nitrate Analyzer. Alliance for Coastal Technology.
Johnson, K.S., Coletti, L.J., 2002. In situ ultraviolet spectrophotometry for high resolution and long-term monitoring of nitrate, bromide and bisulfide in the ocean. Deep Sea Res. Part I 49, 1291–1305.
Kouakou, C.R.C., Poder, T.G., 2019. Economic impact of harmful algal blooms on human health: a systematic review. J. Water Health 17 (4), 499–516.
Ma, P., Zhang, L., Mitsch, W.J., 2020. Investigating sources and transformations of nitrogen using dual stable isotopes for Lake Okeechobee restoration in Florida. Ecol. Eng. 155, 105947.
Mankins, J.C., 1995. Technology Readiness Levels – A White Paper. NASA, Office of Space Access and Technology.
Mathworks, T., R 2022a. MATLAB, 9.12 ed.
Maure, E.R., Terauchi, G., Ishizaka, J., Clinton, N., DeWitt, M., 2021. Globally consistent assessment of coastal eutrophication. Nat. Commun. 12 (1), 6142.
Medina, M., Kaplan, D., Milbrandt, E.C., Tomasko, D., Huffaker, R., Angelini, C., 2022. Nitrogen-enriched discharges from a highly managed watershed intensify red tide (*Karenia brevis*) blooms in southwest Florida. Sci. Total Environ. 827, 154149.
Meyer, D., Prien, R.D., Rautmann, L., Pallentin, M., Waniek, J.J., Schulz-Bull, D.E., 2018. In situ determination of nitrate and hydrogen sulfide in the Baltic Sea using an ultraviolet spectrophotometer. Front. Mar. Sci. 5.
Moscetta, P., Sanfilippo, L., Savino, E.M., Allabashi, R., Gunatilaka, A., 2009. Instrumentation for continuous monitoring in marine environments, OCEANS 2009. Biloxi, MS, p. 9.
NOAA, N.O.a.A.A., 2021. Nutrient and Chlorophyll Monitoring Program and Database Design v1.9. National Estuarine Research Reserves, Centralized Data Management Office ⟨http://www.nerrsdata.org⟩, p. 18.
O'Boyle, Trickett, Partington, Murray, 2014. Field testing of an optical in situ nitrate sensor in three Irish estuaries. Biol. Environ.: Proc. R. Ir. Acad., vol. 114B(no. 1).
Paerl, H.W., Pinckney, J.L., Fear, J.M., Peierls, B.L., 1998. Ecosystem responses to internal and watershed organic matter loading: consequences for hypoxia in the eutrophying Neuse River Estuary, North Carolina, USA. Mar. Ecol. Prog. Ser. 166, 17–25.
Parsons, M.L., Dortch, Q., Turner, R.E., Rabalais, N.R., 2006. Reconstructing the development of eutrophication in Louisiana salt marshes. Limnol. Oceanogr. 51, 534–544.
Pellerin, B.A., Bergamaschi, B.A., Downing, B.D., Saraceno, J.F., Garrett, J.A., Olsen, L.D., 2013. Optical techniques for the determination of nitrate in environmental waters: guidelines for instrument selection, operation, deployment, maintenance, quality assurance, and data reporting: U.S. Geological Survey Techniques and Methods 1–D5. p. 37.
Pellerin, B.A., Bergamaschi, B.A., Gilliom, R.J., Crawford, C.G., Saraceno, J., Frederick, C.P., Downing, B.D., Murphy, J.C., 2014. Mississippi River nitrate loads from high frequency sensor measurements and regression-based load estimation. Environ. Sci. Technol. 48 (21), 12612–12619.
Pellerin, B.A., Stauffer, B.A., Young, D.A., Sullivan, D.J., Bricker, S.B., Walbridge, M.R., Clyde, G.A., Shaw, D.M., 2016. Emerging tools for continuous nutrient monitoring networks: sensors advancing science and water resources protection. JAWRA J. Am. Water Resour. Assoc. 52 (4), 993–1008.
Poornima, D., Shanthi, R., Ranith, R., Senthilnathan, L., Sarangi, R.K., Thangaradjou, T., Chauhan, P., 2016. Application of in-situ sensors (SUNA and thermal logger) in fine tuning the nitrate model of the Bay of Bengal. Remote Sens. Appl.: Soc. Environ. 4, 9–17.
Purcell, K.M., Craig, J.K., Nance, J.M., Smith, M.D., Bennear, L.S., 2017. Fleet behavior is responsive to a large-scale environmental disturbance: hypoxia effects on the spatial dynamics of the northern Gulf of Mexico shrimp fishery. PLoS One 12 (8), e0183032.
Rabalais, N.N., Turner, R.E., 2001. Coastal Hypoxia: Consequences for Living Resources and Ecosystems. American Geophysical Union, Washington, DC.
Rabalais, N.N., Turner, R.E., Justic, D., Dortch, Q., William J. Wiseman, J., 1999. Characterization of Hypoxia: Topic I Report for the Integrated Assessment on Hypoxia in the Gulf of Mexico, Series Analysis Series No. 15. U.S. Department of Commerce. National Oceanic and Atmospheric Administration Coastal Ocean Program, Silver Spring, MD.
Rabalais, N.N., Turner, R.E., Wiseman, W.J., 2002. Gulf of Mexico hypoxia, A.K.A. "the dead zone". Annu. Rev. Ecol. Syst. 33 (1), 235–263.
Reed, M.H., Strope, E.K., Cremona, F., Myers, J.A., Newell, S.E., McCarthy, M.J., 2022. Effects of filtration timing and pore size on measured nutrient concentrations in environmental water samples. Limnol. Oceanogr.: Methods 21 (1), 1–12.

Rieger, L., Vanrolleghem, P.A., Langergraber, G., Kaelin, D., Siegrist, H., 2008. Long-term evaluation of a spectral sensor for nitrite and nitrate. Water Sci. Technol. 57 (10), 1563–1569.
River, M., Richardson, C.J., 2019. Dissolved reactive phosphorus loads to Western Lake Erie: the hidden influence of nanoparticles. J. Environ. Qual. 48 (3), 645–653.
Robertson, D.M., Saad, D.A., 2013. SPARROW models used to understand nutrient sources in the Mississippi/Atchafalaya River Basin. J. Environ. Qual. 42 (5), 1422–1440.
Scavia, D., Rabalais, N.N., Turner, R.E., Justic, D., William, J., Wiseman, J., 2003. Prediction the response of Gulf of Mexico hypoxia to variations in Mississippi River nitrogen load. Limnol. Oceanogr. 48 (3), 951–956.
Schierenbeck, T.M., Smith, M.C., 2017. Path to impact for autonomous field deployable chemical sensors: a case study of in situ nitrite sensors. Environ. Sci. Technol. 51 (9), 4755–4771.
Schnetger, B., Lehners, C., 2014. Determination of nitrate plus nitrite in small volume marine water samples using vanadium(III)chloride as a reduction agent. Mar. Chem. 160, 91–98.
Smith, R.B., Bass, B., Sawyer, D., Depew, D., Watson, S.B., 2019. Estimating the economic costs of algal blooms in the Canadian Lake Erie Basin. Harmful Algae 87, 101624.
Snazelle, T.T., 2015a. Evaluation of Xylem EXO Water-quality Sondes and Sensors: U.S. Geological Survey Open-File Report 2015-1063. p. 28.
Snazelle, T.T., 2015b. Results from Laboratory and Field Testing of Nitrate Measuring Spectrophotometers: U.S. Geological Survey Open-File Report 2015–1065. p. 35.
Spearman, C., 1904. The proof and measurement of association between two things. Am. J. Psychol. 15 (1), 72–101.
Tromboni, F., Dodds, W.K., 2017. Relationships between land use and stream nutrient concentrations in a highly urbanized tropical region of Brazil: thresholds and Riparian zones. Environ. Manag. 60 (1), 30–40.
Turner, R.E., 2001. Of Manatees, Mangroves, and the Mississippi River: is there an estuarine signature for the Gulf of Mexico? Estuaries 24 (2), 139–150.
Turner, R.E., Rabalais, N.N., Justic, D., 2006. Predicting summer hypoxia in the northern Gulf of Mexico: riverine N, P, and Si loading. Mar. Pollut. Bull. 52 (2), 139–148.
Turner, R.E., Rabalais, N.N., Justic, D., 2012. Predicting summer hypoxia in the northern Gulf of Mexico: redux. Mar. Pollut. Bull. 64 (2), 319–324.
USEPA, 1993. Method 365.1, Revision 2.0: Determination of Phosphorus by Semi-Automated Colorimetry.
USEPA, 2013. Reassessment 2013, Assessing Progress Made Since 2008. U.S. Environmental Protection Agency, Washington, DC.
Vuillemin, R., Le Roux, D., Dorval, P., Bucas, K., Sudreau, J.P., Hamon, M., Le Gall, C., Sarradin, P.M., 2009. CHEMINI: a new in situ CHEmical MINIaturized analyzer. Deep Sea Res. Part I: Oceanogr. Res. Pap., vol. 56(no. 8), pp. 1391–9.
Wang, S., Lin, K., Chen, N., Yuan, D., Ma, J., 2016. Automated determination of nitrate plus nitrite in aqueous samples with flow injection analysis using vanadium (III) chloride as reductant. Talanta 146, 744–748.
Wild-Allen, K., Rayner, M., 2014. Continuous nutrient observations capture fine-scale estuarine variability simulated by a 3D biogeochemical model. Mar. Chem. 167, 135–149.
Wilkinson, M.D., Dumontier, M., Aalbersberg, I.J., Appleton, G., Axton, M., Baak, A., Blomberg, N., Boiten, J.-W., Santos, L.Bd.S., Bourne, P.E., Bouwman, i., Brookes, A.J., Clark, T., Crosas, M., Dillo, I., Dumon, O., Edmunds, S., Evelo, C.T., Finkers, R., Gonzalez-Beltran, A., Gray, A.J.G., Groth, P., Goble, C., Grethe, J.S., Heringa, J., Hoen, P.A.Ct, Hooft, R., Kuhn, T., Kok, R., Kok, J., Lusher, S.J., Martone, M.E., Mons, A., Packer, A.L., Persson, B., Rocca-Serra, P., Roos, M., Schaik, Rv, Sansone, S.-A., Schultes, E., Sengstag, T., Slater, T., Strawn, G., Swertz, M.A., Thompson, M., Lei, Jvd, Mulligen, Ev, Velterop, J., Waagmeester, A., Wittenburg, P., Wolstencroft, K., Zhao, J., Mons, B., 2016. The FAIR guiding principles for scientific data management and stewardship. Sci. Data 3, 160018.
Willoughby, S., 2019. Open data and the environment. In: Davies, T., Walker, S., Rubinstein, M., Perini, F. (Eds.), The State of Open Data: Histories and Horizons. African Minds and International Development Research Centre, Cape Town and Ottawa.
Withers, P., Neal, C., Jarvie, H., Doody, D., 2014. Agriculture and eutrophication: where do we go from here? Sustainability 6 (9), 5853–5875.
Wurtsbaugh, W.A., Paerl, H.W., Dodds, W.K., 2019. Nutrients, eutrophication and harmful algal blooms along the freshwater to marine continuum. WIREs Water 6 (5).
Young, N., Sharpe, R.A., Barciela, R., Nichols, G., Davidson, K., Berdalet, E., Fleming, L.E., 2020. Marine harmful algal blooms and human health: a systematic scoping review. Harmful Algae 98, 101901.
Zhang, Y., Wu, L., 1986. Photochemical reduction of nitrate to nitrite in aqueous solution and its application to the determination of total nitrogen in water. Analyst 111, 767–769.